JPE 9-4-4

# Pressure Contact Interconnection for High Reliability Medium Power Integrated Power Electronic Modules

Xu Yang*, Wenjie Chen†, Xiaoyu He*, Xiangjun Zeng*, and Zhaoan Wang*

†*State Key Lab. of Electrical Insulation and Power Equipment, Xi'an Jiaotong University, Shaanxi, China

## ABSTRACT

This paper presents a novel spring pressure contact interconnect technique for medium power integrated power electronics modules (IPEMs). The key technology of this interconnection is a spring which is made from Be-Cu alloy. By means of the string pressure contact, sufficient press-contact force and good electrical interconnection can be achieved. Another important advantage is that the spring exhibits excellent performance in enduring thermo-mechanical stress. In terms of manufacture procedure, it is also comparatively simple. A 4 kW half-bridge power inverter module is fabricated to demonstrate the performance of the proposed pressure contact technique. Electrical, thermal and mechanical test results of the packaged device are reported. The results of both the simulation and experiment have proven that a good performance can be achieved by the proposed pressure contact technique for the medium power IPEMs.

**Keywords:** Pressure contact, Interconnection, Power electronics, Module

## 1. Introduction

Interconnection between power semiconductor and copper traces inside power modules is most important among all issues in packaging for integrated power electronic modules (IPEMs). Pressure contacts using noble metals have been used in packaging high power devices (such as 1800V devices with current ratings of 400A) for a many years [1-3]. The pressure contact device presents the opportunity to exploit the full potential of the incorporated IGBT, due to the close sharing of the voltage and current, plus the close tracking of junction temperature. The elimination of wire and substrate bonds substantially improves the reliability of the IGBT under extreme thermal cycling conditions, representing an improvement even over conventional technology. Pressure contacts yield lower contact resistance than soldered contacts and are less destructive. resistance than soldered contacts and are less destructive. The contact metallurgy, design, and reliability are well understood and proven in a variety of applications, such as SCRs, GTOs or even IGBTs.

However, in medium power module range (power range from several hundred watts to several kilowatts), pressure contacts have never been demonstrated to implement the interconnection between dies and traces inside the module for advanced semiconductor devices such as IGBTs and power MOSFETs [4-7]. It is mainly because the size of the medium

Manuscript received Feb. 19, 2009; revised April 20, 2009
†Corresponding Author: cwj@mail.xjtu.edu.cn
Tel: +86-29-82665223, Fax: +86-29-82665223, Xi'an Jiaotong Univ.
*State Key Lab. of electrical Insulation and Power Equipment, Xi'an Jiaotong Univ.

power module is usually not large enough to permit the use of conventional high strength mechanical blots and springs. In other words, to minimize the volume of the module, aluminum wire bonding is still the dominant technology although many other alternative technologies such as solder bump [9,10], and metallization [8,11] have already been developed. Drawbacks for wire bonding, including high parasitic, reliability issues, have been discussed. What is more fatal is the series process for the technology which becomes an unbreakable bottle neck for mass production.

In view of this, the motivation of this research is to extend the pressure contacts to medium IPEMs range, or in other words, to let pressure contacts give full play in medium power range. At the same time, the disadvantage of wire bonding can be overcome completely. To do this, several new challenges should be considered. One of the most important challenges is: in medium power modules, how to provide enough pressure-contact force without the help of conventional high strength mechanical blots and springs. Another main challenge is how to minimize the contact resistance, which determines the electrical performance of the pressure contact module to a great extent.

In this paper, a novel pressure contact structure utilizing U-shape spring and simple frame structure is presented for medium power integrated power electronic modules with IGBT dies. Electromagnetic performances were evaluated based on both 3D FEA and test results. Reliability for this pressure contact module was tested by temperature cycling tests. A 4kW half bridge module integrated with drivers and control circuits was implemented with pressure contact technology and tested. The results of both the simulation and experiment exhibit promising performances by the proposed pressure contact technique for the medium power IPEMs.

## 2. Materials Design and Package Issue

### 2.1 Structure for pressure contact interconnected modules

The structure for the pressure contact is illustrated in Fig.1. An U shaped spring is used to connect the emitter terminal to the IGBT die. The electrical connection between the spring and the die is guaranteed by contact under the pressure provided by the spring.

The die is attached to the DBC substrate by soldering, although the pressure contact can also be used. The spring is soldered to the emitter plate on top of the module, drivers and controller ICs are mounted on the top side of the emitter plate. The emitter plate and substrate are jointed together with screws, the pressure between the spring and the die is adjusted by fastening the screws and nuts.

The size of the base plate is made by 25 mm×14 mm×4 mm copper. The DBC is 20 mm long, 11 mm wide, with 0.63 mm $Al_2O_3$ ceramic and 0.3 mm thick copper. The size of the copper pad is 8 mm×8 mm×0.8 mm. The thickness of the PCB is 2 mm. The height of the Al wire is 0.8 mm.

### 2.2 Material selection

The material for the spring has to be selected carefully because of the high stress, high temperature and wide temperature cycling operation condition. Beryllium-Copper (BeCu) alloy is selected as the material for the spring because it has high strength, high fatigue-resistance and high thermal conductivity. Also, the spring made of BeCu offers a certain amount of flexibility that helps to reduce thermal stress, compared to other 3D packaging technologies.

To guarantee good electrical contact, and to prevent the spring from corroding and oxidizing as well, the spring is plated with gold. Copper with gold-plate is selected as the material for the transition pad interconnection between the IGBT chip and the spring because of its high thermal conductivity, low electrical resistance and ductile strength to endure thermal stress.

### 2.3 Shape design of the spring

Fig. 2 shows the spring model. It is made by a 0.15mm thick and 6mm wide Beryllium-Copper type and has the

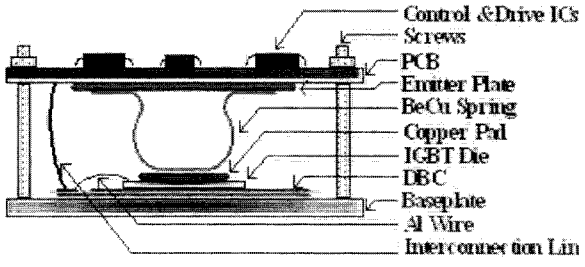


Fig. 1. The cross section of the pressure contact cell.

similar shape as a bubble to provide high elasticity. A 300℃ and 2 hours TSR (Time Stress Relief) process will bring perfect stress performance. TSR refers to a metal thermal management technique in this case. It means putting the metal in room-temperature or a temperature higher than the quenching process in order to improve the strength of the metal.

## 3. Characteristic Analysis of Spring Contact Technique

### 3.1 Mechanical analysis

Distribution of stress on the spring nodes with 3D FEM (finite element method) using ANSYS software is shown in Fig.3. The boundary conditions applied on the key-points forced all nodes of spring moving direction and displacement. Simulation results clarified that the largest stress occurs on the profile surface of the spring.

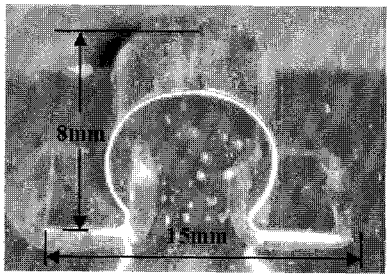


Fig. 2. The photograph of the spring.

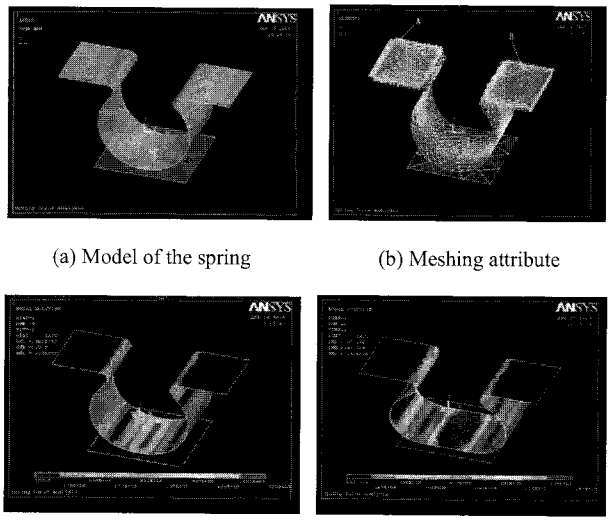


(a) Model of the spring (b) Meshing attribute

(c) Stress distribution under the force of 10N (d) Stress distribution under the force of 40N

Fig. 3. Stress distribution on the spring.

When the spring is used in the pressure contact, two important things must be considered. First, we should avoid the degradation of elasticity of the spring after a long term operation. Second, the spring should provide enough pressurized force in order to minimize the contact impedance. Fig.4 shows the relationship between pressure and displacement on a spring sample. The largest displacement that spring can endure is about 3mm, generated by the force of 40N. The curve drop after 3mm means the elasticity of the spring was totally lost and then fractured.

### 3.2 Contact resistance analysis

A difficult problem of the spring pressure contact technique is contact resistance. The electrical performance of the pressure contact module is seriously affected by contact resistance. The resistance is related to environment temperature, smooth finish of the spring and stress intensity.

Fig.5 illustrates measured resistance of each part between the topside emitter plate and the surface of the IGBT chip as shown in Fig.1. In Fig.5, $R_{AD}$ presents the total resistance of all parts, it is comprised of the spring's bulk resistance ($R_{AB}$), the contact resistance between the spring and the copper pad ($R_{BC}$) and the contact resistance between the pad and Al-sputtered surface of dies ($R_{CD}$). From Fig.5, it can be seen that the contact resistance $R_{CD}$ is the highest point. So how to minimize this contact resistance becomes a critical problem in the module with pressure contact tech.

Fig.6 shows the relationship of conducted voltage drop versus current for the spring pressure contact module and a wire bond module. The voltage drop of the spring module is a little higher than the wire bond module basically because of the contact resistance $R_{CD}$.

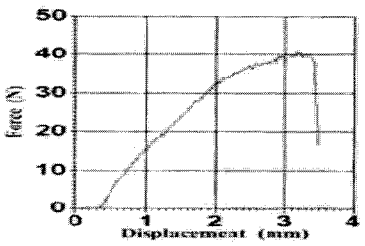


Fig. 4. Characteristic of force versus displacement.

### 3.3 Thermal analysis

Compared to the wire bond technique, the pressure contact package has an additional thermal path: the beryllium-copper alloy spring. To evaluate the thermal performance of the spring, a thermal experiment was carried out to measure the temperature distribution of the module. A total of five thermocouples were mounted in the pressure contact module. The module was mounted onto an Al heat sink with a natural-air cooling approach and the ambient temperature was 33℃. The 25.6W power dissipation was uniformly applied to the IGBT die. After the temperature reached steady state, the thermocouples indicated that the temperature on the top surface of the spring was 58℃, the profile surface of the spring was 60.5℃, the bottom of the spring was 61.3℃, the center point of the base plate surface was 56.5℃ and the edge of the module was 51.5℃.

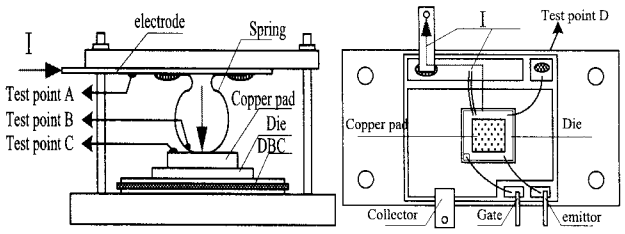


(a) Contact resistance Test platform

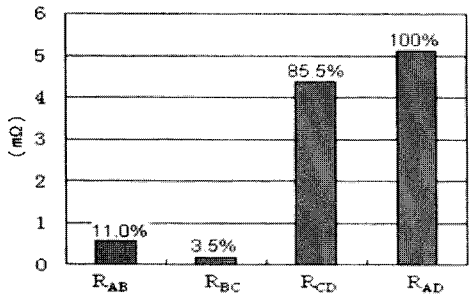


(b) Test results

Fig. 5. Contact resistance of each part.

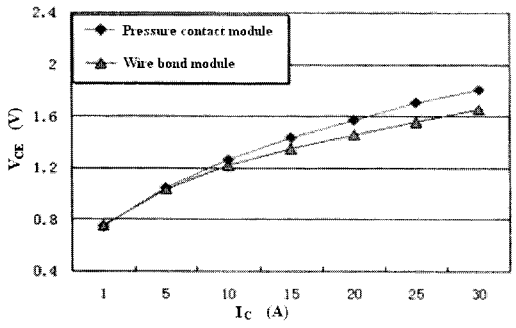


Fig. 6. Conduct voltage drop vs. current.

For a further detection of pressure contact thermal performance, a 3D model was developed using ANSYS under the conditions that used for previous thermal experiment. Using this geometry model, overall temperature distribution of the module is shown in Fig.7. The calculated result shows that the peak temperature of the IGBT chip is 62.934℃.

Pressure contact structure makes double side cooling possible. There are two conduct paths in the module. One is from the IGBT chip to the top-plate through the spring vertically; the other is from the die to the base-plate through the DBC substrate. Although the spring provides an additional thermal path out of the top of the module, the spring has a long and high thermal resistance path. The DBC substrate is the main power dissipation path because of the very short length, large contact area and high thermal conductive ability. The FEM thermal analysis indicated that the thermal resistance of the spring is approximately 43.8℃/W, compared to the DBC of 0.14℃/W. Only 0.4% heat can be removed through the spring and the DBC substrate dissipates about 99.6% of total heat.

### 3.4 Parasitic inductance

The parasitic inductance of the Be-Cu alloy spring was evaluated through parasitic inductance extraction and circuit simulation using Maxwell 3D software. Fig.8(a) shows the geometry model for Ansoft simulation of circuit inductance which consists of line A, B, C and spring D.

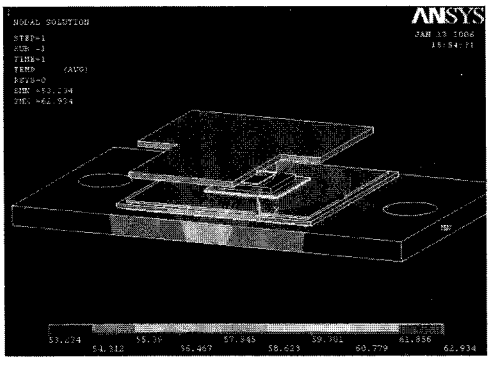


Fig. 7. Temperature distribution of pressure contact structure.

The circuit inductance $L$ could be measured from simulation results. Self-inductance of each line($L_A$, $L_B$, $L_C$) and mutual inductance between line A and B($M_{AB}$) were calculated through PEEC method [12][13]. The mutual inductance between line C and spring D was ignored for the long distance. Therefore the partial equivalent inductance of spring ($L_D$) was calculated under the equation

$$L_D = L - L_A - L_B - L_C + 2M_{AB} \quad (1)$$

In the same way, the wire bond interconnection was also modeled for equivalent parasitic inductance as shown in Fig.8(b).

Fig.9 shows the calculated partial equivalent inductance of the spring related to different frequencies. In contrast to the Al wires, the account of parasitic inductance of the spring is a little bigger.

Fig.10 shows a half-bridge inverter circuit and a low

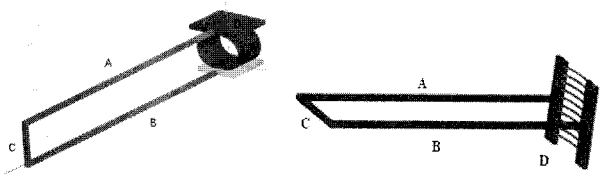


(a) spring circuit (b) Al wire circuit

Fig. 8. Simulation mode.

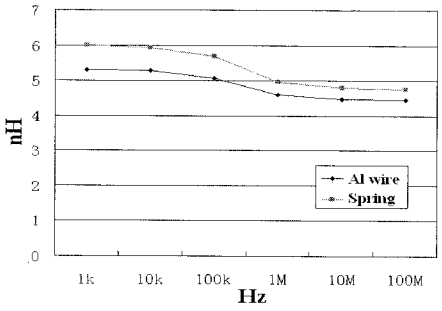


Fig. 9. Calculated results of partial equivalent inductance.

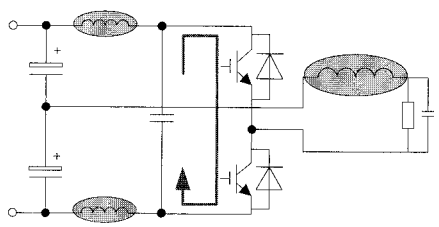

Fig. 10. Half-bridge inverter circuit.

ESL bypass capacitor are connected across the DC bus. When the IGBT is switching on or off, the high di/dt and parasitic inductance will cause large voltage spike and the parasitic resonance causes a high frequency current ringing in the circuit. Because the load inductance, the DC bus parasitic inductance and the impedance of the DC voltage source show large resistance to the high frequency current, the current ringing becomes a circulating current flowing between bypass capacitor and power devices.

Since electromagnetic interference is caused by high frequency voltage or current component, according to the above analysis, it is concluded that the high frequency circulating current flowing through power devices and bypass capacitor is the main magnetic field disturbance source and the parasitic inductance of high frequency current circuit appears to be one of the most important fundamental factors for the electrical performance of the module.

In order to extract the parasitic inductance of critical loop mentioned above, analysis was done through Ansoft Maxwell 3D geometrical simulation as shown in Fig.11. The bypass capacitor could be regarded as a short circuit because of its low impedance for the high frequency current. In the same way, the wire bond module was also modeled. The calculation results are listed in table I, for comparison with the wire bond module's data. The wire bond module used is a commercial IGBT module (IR-PERI GT75TS120K) which has the same power rate as the proposed pressure contact.

Table 1. Calculation results.

| frequency(MHz) | 0.1 | 1 | 10 | 100 |
|---|---|---|---|---|
| Wire bond (nH) | 51.71 | 50.95 | 50.82 | 50.79 |
| Pressure contact (nH) | 143.03 | 142.86 | 142.77 | 142.76 |

It is obvious that the pressure contact module shows a remarkable increment, about 3 times than the amount of the wire bond module in packing parasitic inductance of a high frequency circuit.

It is known from Fig.9 that the increment is not caused by the spring itself. The parasitic inductance is strongly related to the packing structure. In the pressure contact module, for fabricating easily, the low-inductance design

method which is used commonly in commercial IGBT modules is not employed. In future, the structure design of pressure contact module will be optimized, for the reduction of parasitic inductance.

The electrical performance of the pressure contact module was also experimentally evaluated. The experiment circuit is shown in Fig.10 and DC bus voltage is 50V. Fig.12 (a) and (b) present the switching off voltage waveforms. In two kinds of modules, high frequency current ring in the bypass capacitor. The overshoot voltages are 60V (wire bond module) and 75V (pressure contact module). The current ring frequencies are 11.1MHz and 8.92MHz. These tests show the difference between two modules in switching performance. These differences in transient waveforms are attributed to the different packing structures of the modules.

## 4. Configuration Descriptions of IPEM

The pressure contact technique has been implemented in an IPEM. Fig.13 shows the circuit diagram of the module. The half-bridge power switching stage is composed of two IGBTs and two FREDs using pressure contact technique. HCLP-316J is employed as high and low side gate drivers. The driving ICs include function of over current protection and optical coupling isolation inside.

The IPEM is about 92.8mm in length, 34mm in width and 30mm in height. The module has high levels of integration with power semiconductor devices, gate drivers and protection circuits in it. Two IGBT (1200V, 75A) chips and two diodes (1200V, 100A) chips are integrated in this module as demonstrated in Fig.14.

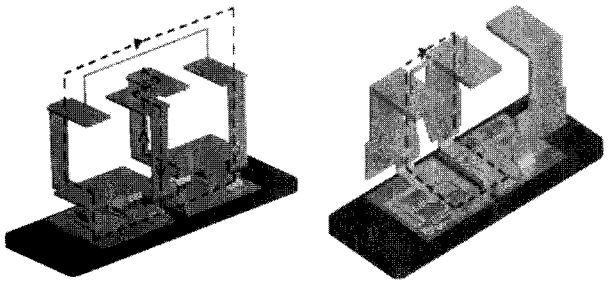

(a)Pressure contact module (b)Wire bond module

Fig. 11. High frequency current circuit mode.

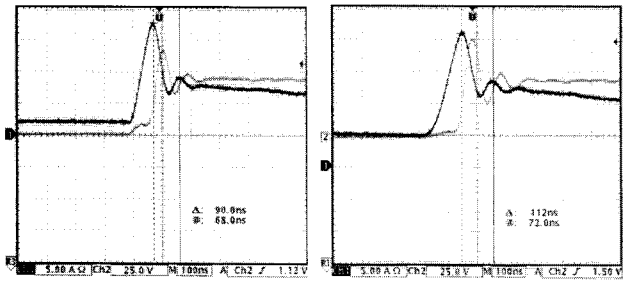

(a) Pressure contact module (b)Wire bond module

Fig. 12. Switching off waveforms.

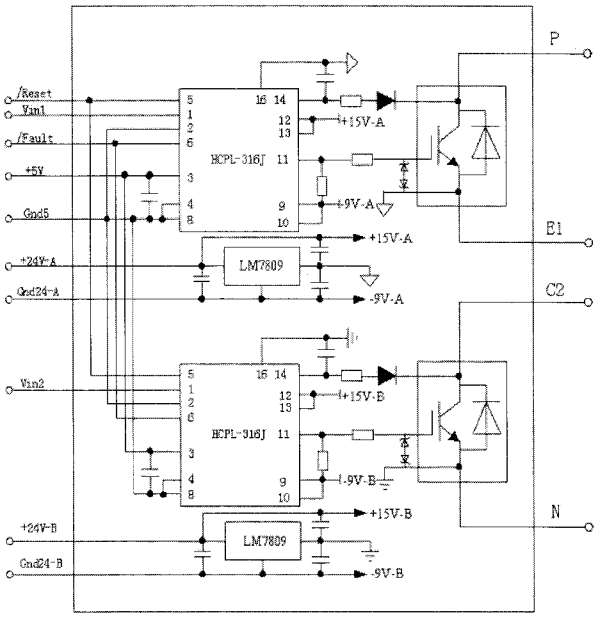


Fig. 13. Circuit schematic for the pressure contact IPEM.

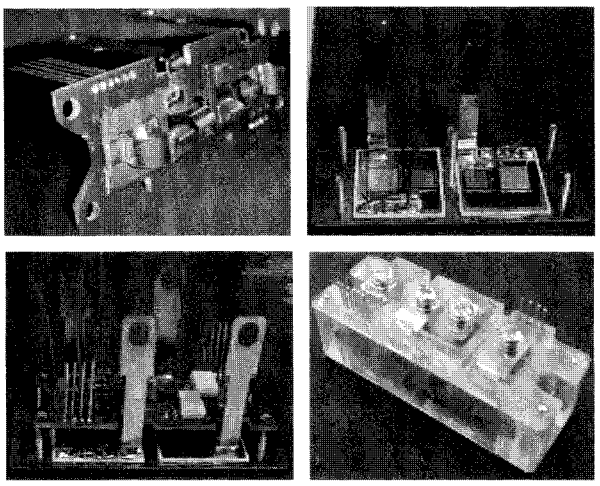

Fig. 14. The photograph of IPEM

## 5. Electrical Testing Results

### 5.1 Reliability evaluation

The CTE mismatching between silicon chip and Al wire in the wire bond module is one of the most important issues in terms of reliability. In the pressure contact module, the spring in elastic range is able to endure the thermo-mechanical stress and the stress concentration on the top surface of the IGBT die vanished.

Thermal cycling tests have been conducted to verify the reliability of the pressure contact packaging. The IGBT module was placed in the thermal cycling test chamber. The temperature changes from -50℃ to 150℃ every 30 minutes. The time for temperature ramp up and ramp down are 5 minutes, respectively. In the remaining 20 minutes of dwell time, the temperature is kept at either -50℃ or 150℃. Tektronix 371B programmable high power curve tracer was used to do the static test. Fig.15 shows the saturation characteristic curves of the pressure contact packaged module before and after 1000 thermal cycles.

The maximum value of Vce was about 1400V before thermal cycling and did not change obviously after 1000 cycles. In contrast to the original value the curve was evidently partial nonlinear and Vce increased little in the saturation area until 1000 cycles.

### 5.2 Power stage result

Experimental evaluation of the power stage test results are shown in Fig.16. The half bridge module is used as a sine-wave inverter. The output of the inverter connects to a LC filter, where $L$=100 , $C$=12 F and $R$=3Ω. The output voltage is about 110V and the output current is about 35.8A, which has reached the design goal of 4kW. The current was detected by 10A:100mV Hall current sensor. After the power stage test, the pressure contact IPEM is still functional and no evident failure could be detected.

## 6. Conclusions

Pressure contact technology has been adopted in high power devices for many years. This paper extended this technology into the interconnection of medium power module to overcome the conventional disadvantages of aluminum wire boning.

To do this, a novel pressure contact interconnect method with the beryllium-copper spring has been preliminarily investigated in this paper. The stress characterization of the spring and the pressure contact performance are studied in detail. It shows that both sufficient press-contact force and good electrical interconnection can be achieved by the proposed method. And the spring exhibits excellent performance in enduring thermo-mechanical stress. A 4 kW half-bridge power inverter module is fabricated to demonstrate the performance of the proposed pressure contact technique The experiment result shows that this method is simple enough and feasible to substitute wire bond technique in medium power IGBT modules or IPEMs.

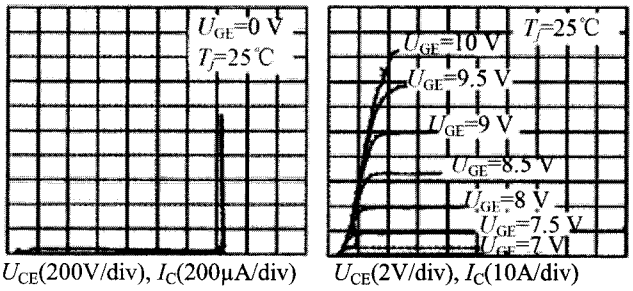


(a) Characteristics before 1000 thermal cycles

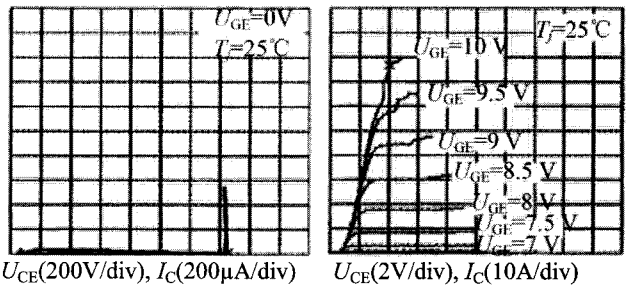


(b) Characteristics after 1000 thermal cycles

Fig. 15. Saturation characteristics curves of module.

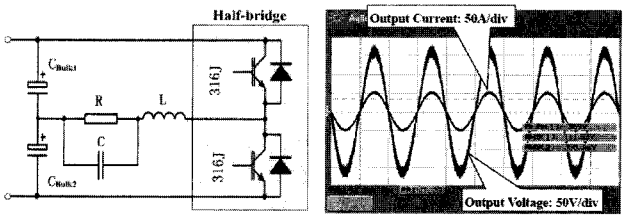


Fig. 16. Power stage results.

## Acknowledgement

This work was supported by the Key Projects in the National Science & Technology of China (2007BAA12B01) and the National Natural Science Foundation of China (NSFC) under Project 50707024.

## References

[1] Chow E.M., Chua C., et al. "Pressure Contact Micro-Springs in Small Pitch Flip-Chip Packages," *IEEE Transactions on Components and Packaging Technologie,* Vol. 29, pp.796 – 803, 2006.

[2] Karnezos M., Pendse R.D., et al. "Reliability of area array pressure contacts on the DTAB package," *IEEE Transactions on Components, Packaging, and Manufacturing Technology*, Part A, Vol.17, pp.263 – 269, 1994.

[3] Beale, J. and Pease R.F. "Limits of high-density, low-force pressure contacts," *IEEE Transactions on Components, Packaging, and Manufacturing Technology*, Part A, Vol.14, pp.257 – 262, 1994.

[4] Woo-Jin, Lee, Seong-Wook, et al. "A New PWM-Controlled Quasi-Resonant Converter for a High Efficiency PDP Sustaining Power Module," *Journal of Power Electronics*, Vol. 7, No. 1, pp.28-37, 2007.

[5] Soon Kurl Kwon, Khairy F. A. Sayed, "Boost-Half Bridge Single Power Stage PWM DC-DC Converters for PEM-Fuel Cell Stacks," *Journal of Power Electronics*, Vol. 8, No. 3, pp.239-247, 2008.

[6] Hang-Seok Choi, "Design Consideration of Half-Bridge LLC Resonant Converter," *Journal of Power Electronics*, Vol. 7, No. 1, pp.13-20, 2007.

[7] Sung-Sae Lee, Sang-Kyoo Han, et al., "A New High Efficiency Half Bridge Converter with Improved ZVS Performance," *Journal of Power Electronics*, Vol. 6, No. 3, pp.187-194, 2006.

[8] Fisher R., Fillion R., Burgess J., and Hennessy W., "High Frequency, Low Cost, Power Packaging Using Thin Film Power Overlay Technology," *in Proc. of IEEE Applied Power Electronics Conference*, pp. 12-17, 1995.

[9] Xingsheng Liu, Xiukuan Jing, and Guo-Quan Lu, "Chip-scale Packaging of Power Devices and its Application in Integrated Power Electronics Module," *in Proc. of IEEE ECTC Conference*, pp. 290-296, 2000.

[10] S. Wen, et al, "Dimple-Array Interconnect Technique for Packaging Power Semiconductor Devices and Modules," *in Proc. of Intemational Symposium on Power Devices and ICs*, pp. 69-74, 2001.

[11] Z.X. Liang, F. C. Lee, G-Q. Lu, and D. Borojevic, "Embedded Power -a multilayer integration technology for packaging of IPEMs and PEBBs", *in Proc. of Internatioal Worshop on Integrated Power Packaging*, pp.41-45, 2000.

[12] Leferink, F.B.J., "Inductance calculations: methods and equations", in Proc. of *IEEE International Symposium Electromagnetic Compatibility*, USA, pp. 16-22, 1995.

[13] Ruehli, A., Paul, C., Garrett, J., "Inductance calculations using partial inductances and macromodels," *in Proc. of IEEE International Symposium Electromagnetic Compatibility*, pp. 23-28, 1995.

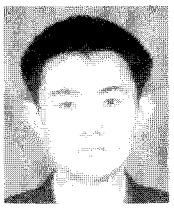

**Xu Yang** was born in China in 1972. He received the B.S. and Ph.D. degrees in electrical engineering from Xi'an Jiaotong University, Xi'an, China, in 1994 and 1999, respectively. He has been a member of the faculty of School of Electrical Engineering, Xi'an Jiaotong University since 1999, where he is presently a Professor. From November 2004 to November 2005, he was with the Center of Power Electronics Systems (CPES), Virginia Polytechnic Institute and State University, Blacksburg,VA, as a Visiting Scholar. He then came back to Xi'an Jiaotong University, and engaged in the teaching and researches in power electronics and industrial automation area. His research interests include soft switching topologies, PWM control techniques and power electronic integration, and packaging technologies.

**Wenjie Chen** was born in Xi'an, China, in 1974. She received the B.S., M.S. and Ph.D. degrees in electrical engineering from Xi'an Jiaotong University, Xi'an, China, in 1996, 2002 and 2006, respectively. She has been a member of the faculty of School of Electrical Engineering, Xi'an Jiaotong University since 2002, where she is currently an Associate Professor. Her main research interests include soft-switching dc/dc converters and active filters, and power electronic integration.

**Xiaoyu He** was born in Tianjing, China, in 1980. He received the B.S. degrees in automatic control from the University of the Tianjing, Tianjing, China, in 2003, and the M.S. degree in electrical engineering from Xi'an Jiaotong University, Xi'an, China, in

2005. He is currently working at China Aerospace science and industry corporation, Beijing, China. His research interests include power electronic integration, packaging technologies and thermodynamic energy processing.

**Xiangjun Zeng** received B.S., M.S. and Ph.D. degrees in electrical engineering from Xi'an Jiaotong University, Xi'an, China, in 1998, 2001 and 2005, respectively. He is currently a lecturer in the School of Electrical Engineering, Xi'an Jiaotong University. From 2006 to 2007, he was with Aalborg University, Denmark, where he was a visiting scholar and was responsible for the development and support of wind power generating technology. His research interests include power electronic integration, wind power generating technology and intelligence testing machines.

**Zhaoan Wang** was born in Xi'an, China, on June 9, 1945. He received the B.S. and M.S. degrees from Xi'an Jiaotong University, Xi'an, China, in 1970 and 1982, respectively, and the Ph.D. degree from Osaka University, Osaka, Japan, in 1989. From 1970 to 1979, he was an Engineer at Xi'an Rectifier Factory. Starting in 1982, he became a Lecturer at Xi'an Jiaotong University, where he is now a Professor. He is engaged in research on power conversion system, harmonics suppression, reactive power compensation and power electronic integration, and active power filters. He has published over 150 technical papers and has led numerous government and industry-sponsored projects in the areas of power and industrial electronics.